Carbohydrate Polymers 87 (2012) 1199–1205

Contents lists available at SciVerse ScienceDirect

Carbohydrate Polymers

journal homepage: www.elsevier.com/locate/carbpol

Modeling and mechanism of the adsorption of proton onto natural bamboo sawdust

Xue-Tao Zhao[a,b], Teng Zeng[a], Zhang Jun Hu[a], Hong-Wen Gao[a,*], Cong Yang Zou[b]

[a] State Key Laboratory of Pollution Control and Resource Reuse, College of Environmental Science and Engineering, Tongji University, Shanghai 200092, People's Republic of China
[b] School of Environmental Science and Engineering, Suzhou University of Science and Technology, Suzhou 215011, People's Republic of China

ARTICLE INFO

Article history:
Received 20 June 2011
Received in revised form 30 August 2011
Accepted 31 August 2011
Available online 8 September 2011

Keywords:
Bamboo sawdust
Surface complexation model
Pznpc

ABSTRACT

Natural bamboo sawdust with cellulose–lignin polymeric structure was used as a raw adsorbent to remove heavy metal and dyes in water. The analysis of surface properties showed that high proton affinity sites were mainly composed of phenolic and alcohol hydroxyl, while low proton affinity sites mainly consisted of carboxylic acid, silicon hydroxyl, aluminum hydroxyl and some low densities of sulfhydryl and phosphoryl groups. The results fitted by NEM surface complexation model showed: three-sites model fitted acid–base titration data better than two-sites and one-site model. Acid–base titration experiments showed the amount of acid and base consumed was not uniform between acid and alkali side. This was probably due to the swelling of cellulose in acid side, but the possibility that different reactions occurred in acid and alkali side cannot be completely excluded. Pznpc of sawdust was between pH 5.2 and 5.5.

1. Introduction

With the rapid development of modern industry, the discharge of heavy metal and dye wastewater from the production process has become a major environmental concern. The treatment of low-concentration wastewater is often difficult. As such, adsorption becomes an alternative and has grown into one of the most versatile processes. The most widely used adsorbent is activated carbon. However, its operation and maintenance cost is relatively high. Recently, abundant research has been conducted to seek more cost-effective adsorbents for the removal of pollutants. Sawdust is one of the promising materials which can be used to adsorb heavy metals (Ahmed, 2011; Lee, 2001; Naiya, Hattacharya, & Das, 2008; Sciban, Radetic, Kevresan, & Klašnja, 2007;Shukla, Zhang, Dubey, Margrave, & Shukla, 2002; Yasemin & Zek, 2007), dye (Batzias & Sidiras, 2005; Ferrero, 2007; Ofomaja, 2008; Özacar & Şengil, 2005) and some other organic contaminants (Ofomaja & Unuabonah, 2011; Ye et al., 2010) from water.

To better understand the adsorption of metal ions and dyes on natural sawdust, detailed information is required on the constitutive moieties of functional groups involved in the complexation reactions. The sorption characteristics of sawdust strongly depend on its charging status controlled by the types and numbers of functional groups on its surface. In this paper, surface complexation model was used to account for the surface property and reactivity of sawdust because it offered a specific mechanism by explaining surface chemical reactions with a set of thermodynamic constants. This model has been successfully applied to explain the sorption reaction of natural polysaccharide (Guo, Zhang, & Shan, 2008; Reddad, Cerente, Andres, & Clolrec, 2002), and wheat bran (Ravat, Dumonceau, & Monteil-Rivera, 2000).

It is well known that the binding of proton and metal ions and dyes are closely related (Ravat et al., 2000). But few research was conducted to study the proton binding property of sawdust. Natural bamboo sawdust is mainly composed of cellulose, hemicellulose and lignin. Among them, cellulose and hemicellulose, which account for about 50% of the dry matter, are complex carbohydrate polymers as the major constituents. The study not only lays the theoretical ground for the application of other sawdust adsorption materials, but also provides reference for that of agricultural waste with cellulose or lignin as the main components, such as waste tea leaves (Ahluwalia & Goyal, 2005), rice bran (Montanher, Oliveira, & Rollemberg, 2005; Singh, Rastogi, & Hasan, 2005; Sud, Mahajan, & Kaur, 2008;), bran shell, coconut fiber (Shukla & Pai, 2005) and cob (Khan & Wahab, 2006; Ngah & Hanafiah, 2008) in heavy metal removal and apple pomace, wheat straw (Robinson, Chandran, Naidu, & Nigam, 2002) and husk (Robinson, Chandran, & Nigam, 2002) in dyes removal.

In contrast to most other plants which need to grow for 10–100 years, bamboo is a fast-growing and renewable resource, which becomes mature in 4–6 years. Additionally, the wood processing in industrial and agricultural production often generates a massive amount of sawdust that needs to be reused. In view of this, we choose bamboo sawdust as a natural adsorbent for study. Bamboo sawdust used in this study is not chemically modified to maintain its low cost.

* Corresponding author. Tel.: +86 02165988598; fax: +86 02165988598.
E-mail address: emsl@tongji.edu.cn (H.W. Gao).

0144-8617/$ – see front matter © 2011 Elsevier Ltd. All rights reserved.
doi:10.1016/j.carbpol.2011.08.098

Table 1
Acid–base titration surface complexation reaction.

Species	Mass action relation	Equilibrium constant	
$>XOH_2^+$	$>XOH + H^+ \Leftrightarrow >XOH_2^+$	K_1^+	(2)
$>XO^-$	$>XOH \Leftrightarrow >XO^- + H^+$	K_1^-	(3)
$>YO^-$	$>YOH \Leftrightarrow >YO^- + H^+$	K_2^-	(4)
>ZH	$>Z^- + H^+ \Leftrightarrow >ZH$	K_{ZH}	(5)
>ZK	$>ZH + K^+ \Leftrightarrow >ZK + H^+$	K_{ZK}	(6)
>ZH	$>ZK + H^+ \Leftrightarrow >ZH + K^+$	K_{ZH}	(7)

2. Materials and methods

Bamboo sawdust was obtained from a timber mill in South China. Bamboo sawdust was dried in an oven at 70 °C for 24 h, and then grounded and screened through a set of sieves to get particles with geometrical size from 100 to 200 μm.

2.1. Acid–base titration

Experiments were fully automated by computer-controlled Metrohm 798 microprocessor pH meter. All potentiometric titration experiments were performed in a thermo-stated cell at 22 ± 1 °C under a nitrogen stream, using a glass electrode paired with an internal calomel electrode. One gram of sawdust was added into a 100 mL beaker and fully mixed with 50 mL 0.01, 0.1 or 1 M KNO_3 solution. The pH of solutions under different ionic strength was approximately 5.5 (acid side starting point). The sawdust suspension was first titrated to pH 3.5 (alkali side starting point) by HNO_3 solution and then to pH 10.5 by KOH solution. The titration rate was adjusted with a stability criterion of less than 0.01 pH unit. The total titration time was approximately 5 h. With the same titration method, the above experiments were repeated with no addition of sawdust.

2.2. Sawdust chemical and physical properties analysis

The elements and their contents in sawdust were analyzed by X-ray fluorescence (SRS3400 type, Bruker AXS corporation in Germany).

Infrared spectral analysis was done by using solid presser method. The data from 500 to 4000 cm^{-1} spectral range was collected by an infrared spectrometer (Nicolet 5700, Nicolet company in USA). Nine alkali side experimental data points of titration experiment were used for Zeta potential analysis. After titration, the pH of suspension was measured by pH meter and the supernatant was removed for zeta potential measurements after 10 min by zeta potential analyzer (Zetasizer Nano Z type, Malvern Instruments Ltd.).

3. Results and discussion

Since constant capacity model, diffusion layer model and three layer model were unable to fit the data well, this paper adopted the non-electrostatic model (NEM) (Kohler, Curtis, David, Meece, & Davis, 2004; Marmier & Fromage, 1999) to fit the data. Equilibrium constants and mass action relation were summarized in Table 1.

3.1. At alkali side with pH 3.5 as the starting point for the model fitting

When pH 3.5 was chosen as the starting point for data analysis and fitting, the charge variation of surface protons (mol/kg) resulting from the combination of H^+ or OH^- can be expressed as:

$$\Delta Q = \frac{-V_{OH}C_{OH} + V_{OHK}C_{OH}}{(V_0 + V_H + V_{OH})C_s} \quad (1)$$

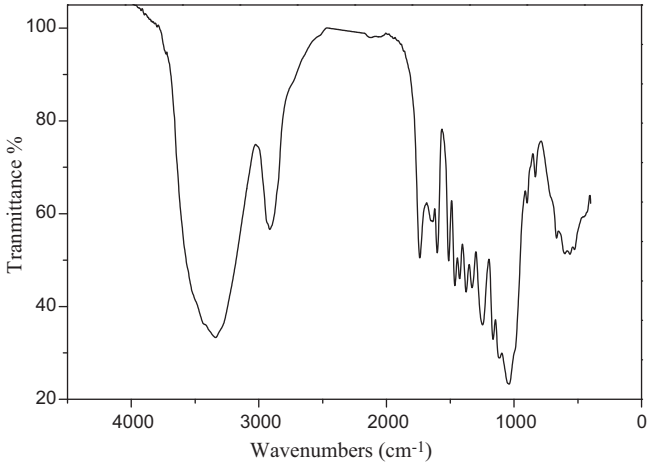

Fig. 1. Infrared spectra for natural bamboo sawdust.

where V_{OH} and V_H were acid and base volume (mL) added during titration, respectively. V_{OHK} was the base volume (mL) added during blank titration. C_{OH} was the base concentration (mol/L), V_0 was the initial volume of suspending liquid (mL), C_s was the sawdust concentration of suspending liquid (kg/L).

From infrared spectra (Fig. 1), the following conclusions were drawn: 3200–3600 cm^{-1} wide peak resulted from hydroxyl peak (including phenolic hydroxyl, alcohol hydroxyl of sawdust and water molecules) (Gode, Atalay, & Pehlivan, 2008), 2920 cm^{-1} peak can be attributed to methyl, methylene group and the extension vibration of C–H bond in the aromatic methoxyl group. 1641 and 1740 cm^{-1} corresponded to the vibration range of carbonyl groups. It had been shown that 1740 cm^{-1} was the free carbonyl stretching vibration of carboxylic acid group and 1641 cm^{-1} was the potentiometric anionic stretching vibration (Bouanda, Dupont, Dumonceau, & Aplincourt, 2002). 1602, 1425, 1511 cm^{-1} were characteristic of aromatic main structure vibration. Both 1517 and 1467 cm^{-1} were the deformation vibration of methoxy group on aromatic ring. 900, 1050 and 1384 cm^{-1} can be inferred as carbohydrate characteristic peaks. 835, 1045, 1160 and 1251 cm^{-1} should be guaiacyl characteristic peaks (Tejado, Pen, Labidi, Echeverria, & Mondragon, 2007), 1122 and 1330 cm^{-1} should be syringyl characteristic peaks and both of them were lignin endemic components. 1602, 1425 (Guo et al., 2008), 1511, 1467 and 1517 cm^{-1} all exhibited the main structure characteristics of aromatic ring, but only 1641 and 1740 cm^{-1} showed the unique structure of carboxylic acid groups. This suggests that phenolic groups and alcohol hydroxyl groups are more abundant than carboxylic acid groups in sawdust.

Sawdust surface contained a large number of hydroxyl groups. If the energy of these groups was equivalent, then only one type of surface functional group (in this case, XOH) participates in the reaction. Eq. (2) in Table 1 was a protonation reaction, while Eq. (3) was a deprotonation reaction. This was the so-called one-site model. In fact, the energy of different sawdust surface groups was significantly different and can be categorized into two types: low proton affinity sites (in this case, XOH) and high proton affinity sites (in this case, YOH). According to Fig. 1, low proton affinity sites generally referred to carboxylic acid group, while high proton affinity sites generally referred to alcohol hydroxyl and phenolic groups. This was the so-called two-sites model. Relatively, the proton at high proton affinity sites can be abstracted more hardly. Also, alcohol hydroxyl and phenolic hydroxyl groups were more difficult to be protonated, so their protonation reactions are negligible. Their deprotonation reaction was shown by Eq. (4).

Certainly, other types of affinity sites may also exist. The main components of sawdust were cellulose, hemi-cellulose and lignin

(Lee, 2001), which contained over 99% of C, H, O. By X-ray fluorescence analysis, other elements with atomic number higher than 8 included Si (0.21%), Al (0.49%), K (0.15%), S (0.11%), P (0.035%), Cl (0.024%), Zn (0.023%), Mn (0.0046%), Ca (0.0019%), and Fe (0.0011%). These elements can form >AlOH, >SiOH, >SH, $>PO_3H$, etc. These groups, especially >SH and $>PO_3H$, were often present at low abundance, so it was difficult to locate their characteristic peaks in infrared spectrum.

The cellulose in sawdust was crystalline, while lignin was amorphous (Lee, 2001). Due to the semi-crystal characteristic of sawdust, it may possess some properties that can only be found on crystal. Therefore, some lattice defects may exist in its structure, which led to the presence of permanent charge. According to the research on mineral crystals, these permanent charges were generally negatively charged, and tended to participate in ion exchange reaction (Anderson & Sposito, 1991; Chu, 2003). Three-sites model was therefore proposed as an improvement of two-sites model by incorporating the ion exchange reaction of permanent charge. These ion exchange sites bound with hydrogen ions in acid side titration (Eq. (5)) or exchanged with potassium ions (in the presence of KNO_3) in alkali side titration (Eq. (6)).

Using Eq. (1), ΔQ was calculated with varying pH and ionic strength (Fig. 2). Different site model was applied to fit data and results were summarized in Table 2 and Fig. 2. Using FITEQL software (Herbelin & Westall, 1999), Fig. 3 was obtained which showed the change of surface species with varying pH according to fitting parameters in Table 2. From Table 2 and Fig. 2, the more sites, the better the data were fitted (in one-site model fitting, protonation reaction was excluded). Among all fittings, one-site model gave worst fitting. Its WSOS/DF (Herbelin & Westall, 1999; Westall, Jones, & Gary, 1995) ratio was higher than 1000. This reflected that the hydrogen ion adsorption capacity of sites on sawdust varied substantially.

Two-sites model fitted better. Its WSOS/DF ratios dropped to 65 or so. Except for $\log K_1^+$, the values of fitting parameters under different ionic strengths only changed slightly, suggesting a similar proton binding mechanism. For low proton affinity sites, $\log K_1^-$ was between −4.70 and −4.8, whereas its value was between −9.3 and −9.6 for high protons affinity sites. As shown in Fig. 3A–D, the trend in the change of site density of surface species was also roughly the same as pH changes. For example, in Fig. 3A, the numerical value of XOH_2^+ was very small when pH was above 3.5 and therefore can be neglected. Despite the change of $\log K_1^+$ was remarkable in two ionic strength series, it has no significant impact on fitting results of other data. As pH rose, XOH site density decreased gradually, while XO^- site density increased gradually. At pH 4.75, XO^- and XOH site density equaled to each other, resulting in a continuous increase in XO^- until a maximum threshold was reached (i.e. the T(XOH) 0.0381 mol/kg in Table 2). T(XOH) was the sum of XOH_2^+, XOH and XO^- site density and their relative proportion only changed with pH. When pH was higher than 6, low

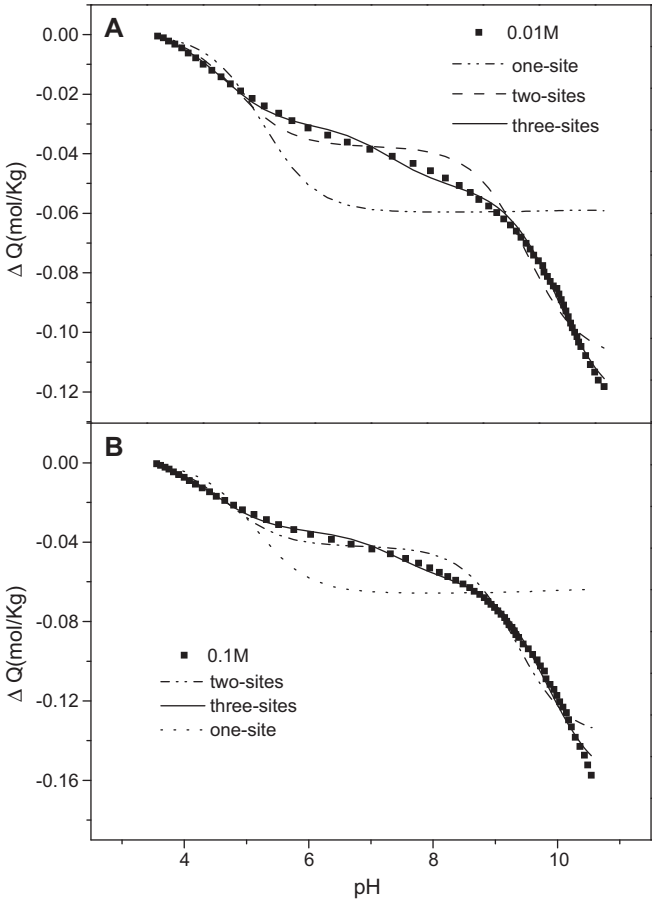

Fig. 2. ΔQ–pH fitting curve of Surface complexation models under different ionic strengths. (A) 0.01 M KNO_3 and (B) 0.1 M KNO_3.

proton affinity sites existed in the form of XO^-, as all protons have dissociated. Also, from Fig. 3A–D the density of high proton affinity sites was much higher than that of low protons affinity sites. These results were in agreement with infrared spectrum, in which alcohol hydroxyl and phenolic hydroxyl group peaks had a higher intensity than carboxylic acid peak. When pH was less than 7, surface species were in the form of YOH. Proton did not dissociate from sites until pH was raised above 8. At pH higher than 8, YO^- concentration gradually increases but did not reach a plateau during titration. For ion exchange sites, when pH was below 5.5, ZH predominated; when pH was above 5.5, ion exchange reaction started to occur; when pH was above 9, ZK became dominant.

From Table 2 and Fig. 2, three-sites model fitted data better than two-sites model. Since pH 3.5 was used as the starting point for data fitting, three-site model incorporated Eq. (6) instead of Eq. (5). The

Table 2
Fitting parameters of surface complexation model.

Model	$\log K_1^+$	$\log K_1^-$	$\log K_2^-$	$\log K_{ZK}$	$\log K_{ZH}$	T(XOH) (mol/kg)	T(YOH) (mol/kg)	T(ZK/ZH) (mol/kg)	WSOS/DF
0.01 M									
One-site		−5.27				0.0605			1.03E+03
Two-sites	0.531	−4.82	−9.51			0.0381	0.074		63.6
Three-sites	2.32	−4.66	−10.0	−7.30		0.0310	0.0800	0.0209	7.32
Three-sites (1)	3.99	−5.46	−10.1		7.83	0.0211	0.0788	0.0170	9.07
Three-sites (2)	4.84	−9.13	−10.7		6.99	0.0314	0.0917	0.0126	13.3
0.1 M									
One-site		−5.14				0.0668			1.12E+03
Two-sites	2.08	−4.72	−9.36			0.0427	0.104		64.9
Three-sites	2.42	−4.53	−9.86	−7.39		0.0350	0.115	0.0249	8.25
Three-sites (1)	3.78	−5.20	−9.82		7.62	0.0239	0.112	0.0203	12.0
Three-sites (2)	4.64	−8.95	−10.4		7.00	0.0357	0.130	0.0156	10.7

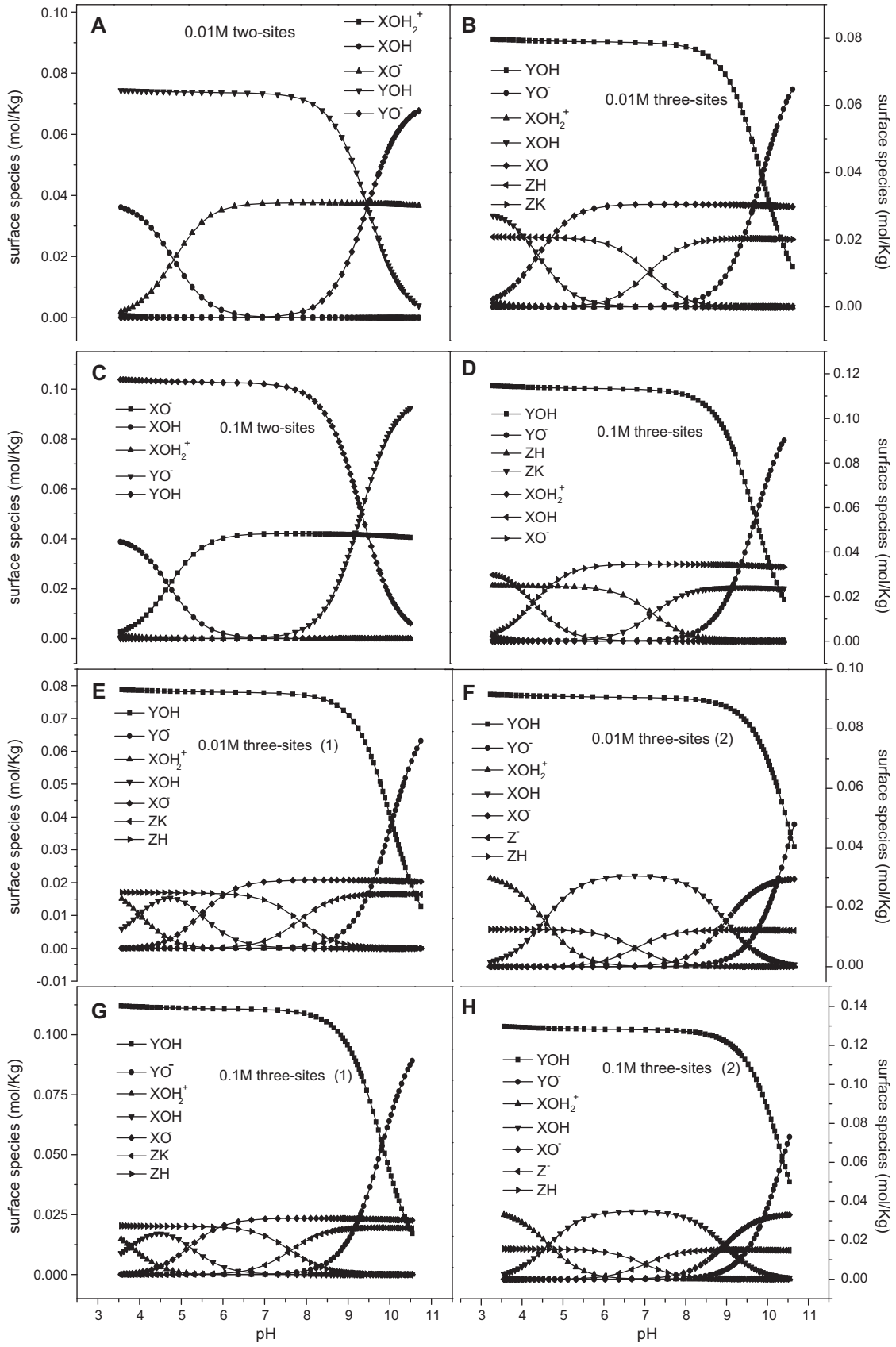

Fig. 3. The predicted distribution of surface species of sawdust with the change of pH under different ionic strength. (A) 0.01 M KNO_3 two-sites, (B) 0.01 M KNO_3 three-sites, (C) 0.1 M KNO_3 two-sites, (D) 0.1 M KNO_3 three-sites, (E) three-sites (1) 0.01 M KNO_3, (F) three-sites (2) 0.01 M KNO_3, (G) three-sites (1) 0.1 M KNO_3, and (H) three-sites (2) 0.01 M KNO_3.

Table 3
Material balance coefficient of three sites surface complexation models.

Species	>XOH	>YOH	>ZK/>ZH	H^+	Model
>ZH	0	0	1	0	Three-sites
>ZK	0	0	1	−1	
>ZK	0	0	1	0	Three-sites (1)
>ZH	0	0	1	1	
$>Z^-$	0	0	1	−1	Three-sites (2)
>ZH	0	0	1	0	

mass balance matrix in Fiteql software (Herbelin & Westall, 1999) are summarized in Table 3. Because >ZK represents the loss of a hydrogen ion, >ZK and >ZH in the "H^+" column are designated as "−1" and "0", respectively.

Compared to two-sites model, the fitting parameters of three-sites model did not change too much, so the two-sites model may basically be able to explain the binding mechanism between hydrogen ions and sawdust. The absolute value of $\log K_1{}^-$ of three-sites model fitting was slightly lower than that of two-site model, while the absolute value of $\log K_2{}^-$ was slightly higher. Correspondingly, site densities T(YOH) of three-sites model was higher with lower T(XOH). This reflected the interdependence of these parameters. Take "0.1 M" as an example, $\log K_2{}^-$ for three-site model was −9.86, which meant more high proton affinity surface sites were involved in adsorption, so T(YOH) was also a bit higher. T(XOH) became lower because some low proton affinity sites were attributed to ion exchange reaction of permanent charge. In three-sites model, the density of new ion exchange sites was about two-thirds of that of low proton affinity sites, indicating the importance of this reaction. Two-sites model did not reflect this consideration, and therefore gave a lower WSOS/DF ratio.

3.2. At acid side with pH 5.5 as the starting point for the model fitting

Surface protons charge (mol/kg) resulting from sawdust surface binding H^+ or OH^- can be given by Eq. (8), where (H^+) and (OH^-) were hydrogen ion and hydroxyl ion concentrations before titration, respectively, V_{HK} and V_{OHK} were acid and base volumes added during the blank titration, respectively, C_H and C_{OH} were acid and

$$Q = \frac{\{(V_H C_H - V_{OH} C_{OH} - (V_{HK} C_H - V_{OHK} C_{OH}))/(V_0 + V_H + V_{OH}) + [OH]^- - [H]^+\}}{C_s} \quad (8)$$

Alkali concentrations (mol/L), respectively. V_H, V_{OH}, V_0 and C_s were the same as in Eq. (1). According to Eq. (8), Fig. 4A was obtained.

Sawdust surface reactions were more complicated than expected. When performing the acid–base titration analysis, an interesting phenomenon was observed. Using same concentration and volume of acid and base, the amount of acid used to titrate from initial pH 5.5 down to pH 3.5 was always a bit more than that of base used to titrate back from pH 3.5 to pH 5.5. For example, in 0.01 M KNO_3 system, the acid side used 18 drops, while alkali side only used 16 drops; in 0.1 M KNO_3 system, acid side used 20 drops, while alkali side only used 17 drops. Theoretically, if the reaction was fully reversible, the amount of acid and base used should be the same. Two possibilities can explain such difference.

Firstly, under acidic conditions, swelling can occur in the cellulose and hemi-cellulose components of sawdust (Lee, 2001). Thus, sawdust may absorb more hydrogen ions in acid side titration. Before titration, sawdust was soaked in KNO_3 solution of high concentration, so the negatively charged site would bind with potassium ions to form >ZK. Then the ion exchange reaction in acid side proceeded following Eq. (7), while ion exchange reaction in alkali side proceeded following Eq. (6). Eqs. (6) and (7) are reversible. The excess acid consumed in acid side can be explained by cellulose swelling.

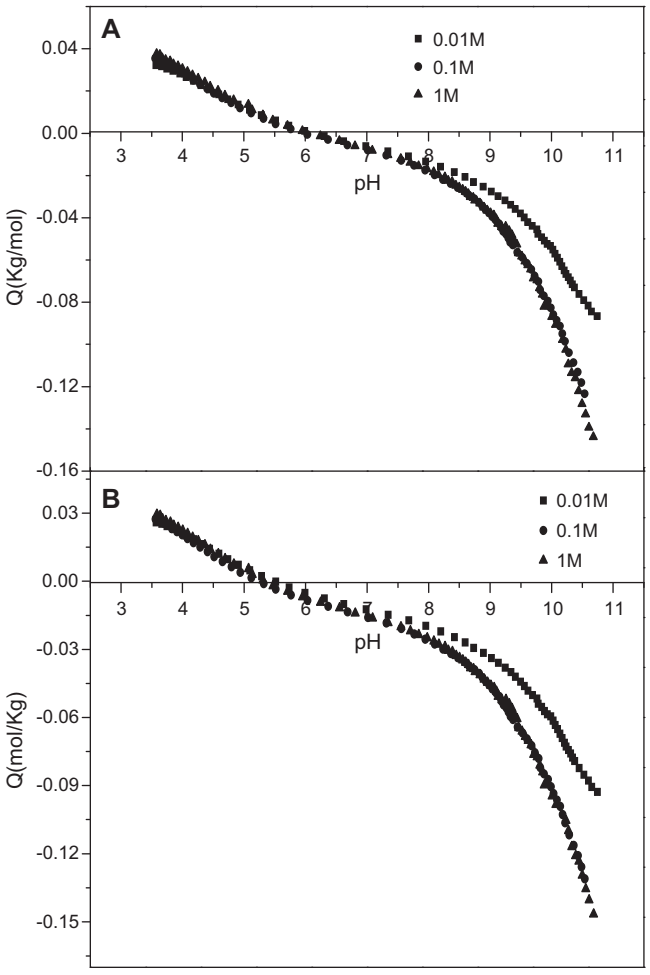

Fig. 4. (A) Surface proton charge Q curve with the change of pHB. (B) Surface proton alkali equivalent charge Q curve with the change of pH.

The second explanation was that two different reactions occurred in acid side and alkali side. In acid side the reaction followed Eq. (5), whereas in alkali side the reaction followed Eq. (6). The difference was that no potassium ion participated in the reaction of acid side. The data was fitted individually and the fitting results were summarized in Table 2. Three-sites (1) represented the first possibility, and three-sites (2) represented the second possibility.

From Table 2, three-sites (2) model and three-sites (1) model yield comparable fitting results. Both of them fitted data reasonably well. As for three-sites (1) model (see Table 3), when >ZK was the initial state, "H^+" was designated as "0"; when >ZH obtained a proton, "H^+" changed its value to "1". As for three-sites (2) model, when $>Z^-$ was the initial state, "H^+" was "−1"; when> ZH obtained a proton, "H^+" changed to "0".

The change in the distribution of surface species with pH for three-site (1) was analogous to Fig. 3A–D in addition to a sharp increase in "$XOH_2{}^+$" concentration (Fig. 5E and G). This was caused by taking pH 5.5 as the starting point for fitting. In addition, although the absorption of excess hydrogen ions due to sawdust swelling was not necessarily attributed to the reaction $XOH + H^+ \rightarrow >XOH_2{}^+$, the hydrogen ions absorbed can only be explained by the surface complexation model, reflect-

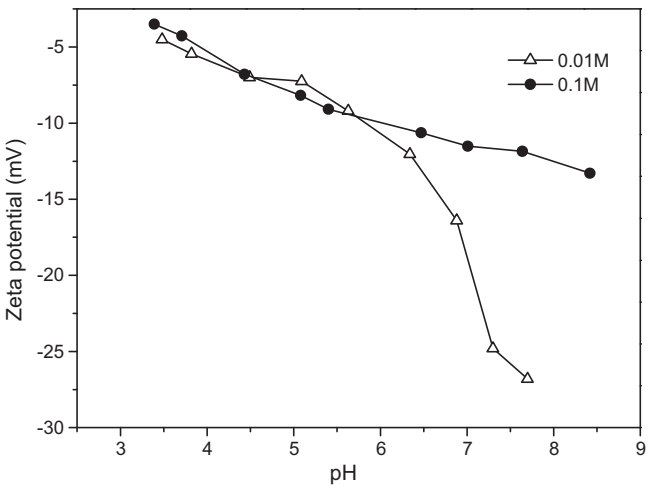

Fig. 5. Zeta potential with the change of pH and ionic strength.

ing the increase of "XOH_2^+" concentration. Meanwhile, $\log K_1^+$ value increased as the increase of "XOH_2^+" concentration. This was because the importance of formula (2) boosted because of increased data points of acid side. $\log K_1^+$ also reached 3.5 above. In contrast, $\log K_1^+$ was normally lower than 3.5 for by taking pH 3.5 as the starting point for fitting, and "XOH_2^+" concentration only slightly affected fitting data.

Under different ionic strengths, the absolute value of $\log K_{ZH}$ of three-site (1) was roughly the same as $\log K_{ZK}$ in Table 2, but the sign was opposite. This was because Eqs. (6) and (7) were the reversible reaction of each other. $\log K_2^-$ and T(YOH) did not change significantly with the change of fitting starting point as other parameters did. These changes reflected the interdependence of these parameters.

$\log K_{ZH}$ fitting values of three-site (2) model were slightly smaller than those of three-sites (1) model, suggesting that the difference between reactions (5) and (7) is small. It appeared that whether potassium ion participates in the reaction was not critical. But from Table 3, the value of "H^+" of reactions (5) and (7) were significantly different from each other, causing great changes in other fitting parameters and the distribution of surface species (Fig. 3E–H). $\log K_1^-$ and $\log K_2^-$ in three-sites (2) model were very close, indicating that this model was not sufficiently sensitive to distinguish low proton and high proton affinity sites.

Based on the fitting results, it was hard to tell which possibility is more likely to occur. But under acidic conditions, cellulose swelling was widely known (Lee, 2001), so the first possibility seemed to be more reasonable. Or at least, the actual reaction of sawdust in acid side can be explained by taking both possibilities into account. For ordinary adsorbents, the choice of starting point did not affect the subsequent fitting of metal ion adsorption. But in this study, in order to eliminate the potential errors, the fitting data with alkali side pH 3.5 as starting point were chosen for the subsequent metal ions adsorption fitting in several future papers.

3.3. The study on the charge of sawdust surface

In theory, with increasing ionic strength, the diffusion layer should be compressed, leading to a smaller absolute value of zeta potential. This was well supported by experimental results shown in Fig. 5. Additionally, though the negative charges on surface diminish with decreasing pH, the sawdust had always be negatively charged. Therefore, the zero charge point (Pzc) (Sposito, 1998) and the isoelectric point (Iep) of sawdust cannot be determined because a large proportion of permanent charge was not involved in reaction.

According to formula (8) and Fig. 4A, in 0.01 M, 0.1 M and 1 M KNO_3 systems, the corresponding pH values are 6.13, 5.97, 6.09 when $Q = 0$, respectively. Even if the effect of KNO_3 on the surface charge was assumed to be negligible, these pH values cannot be viewed as net protons zero charge points (PZNPC) (Sposito, 1998). This was because these hydrogen ions which swelling sawdust tended to absorb, or which were abstracted from permanent charges should not be considered as the coordination charge. If the amount of acid used in acid side was replaced by corresponding alkali equivalence in alkali side, a new Q value can be recalculated by formula (8) and the results are plotted (Fig. 4B). The new Q value excluded the excess acid absorbed in acid side. In 0.01 M, 0.1 M and 1 M KNO_3 systems, the corresponding pH values when $Q = 0$ are 5.49, 5.25 and 5.41, respectively. These values were considered as Pznpc of sawdust. In addition, below pH 6, T(YOH) and T(ZK) of three-sites (1) model mainly existed in the form of YOH and ZH, so the charge of surface site largely depended on XO^- and XOH_2^+.

4. Conclusion

The surface properties analysis showed that semi-crystal properties existed in the structure of sawdust. The results fitted by NEM surface complexation models with alkali edge pH 3.5 as the starting point showed: three-sites model fitted data better than two-sites and one-site model. Pzc and Iep of sawdust cannot be determined and Pznpc was between pH 5.2 and 5.5. Based the above study result, the extension of this study to metal ion and dyes adsorption will be presented in several future papers.

Acknowledgements

The work was supported by funds from the National Key Technology R&D Program of China (Grant no. 2008BAJ08B13).

References

Ahluwalia, S. S., & Goyal, D. (2005). Microbial and plant derived biomass for removal of heavy metals from waste water. *Bioresource Technology*, *B98*, 2243–2257.
Ahmed, S. A. (2011). Batch and fixed-bed column techniques for removal of Cu(II) and Fe(III) using carbohydrate natural polymer modified complexing agents. *Carbohydrate Polymers*, *83*, 1470–1478.
Anderson, S. J., & Sposito, G. (1991). Cesium adsorption method for measuring accessible structural surface charge. *Soil Science Society of America Journal*, *55*, 1569–1576.
Batzias, F. A., & Sidiras, D. K. (2005). Dye adsorption by prehydrolysed beech sawdust in batch and fixed-bed systems. *Bioresource Technology*, *98*, 1208–1217.
Bouanda, J., Dupont, L., Dumonceau, J., & Aplincourt, M. (2002). Use of a NICA – Donnan approach for analysis of proton binding to a lignocellulosic substrate extracted from wheat bran. *Analytical and Bioanalytical Chemistry*, *373*, 174–182.
Chu, Z. S. (2003). *Surface characteristics of Chinese loses and its reaction mechanisms and models with metal ions*. Ph.D. Dissertation, Research Center for Eco-Environmental Sciences, Chinese Academy of Sciences, Beijing.
Ferrero, F. (2007). Dye removal by low cost adsorbents, Hazelnut shells in comparison with wood sawdust. *Journal of Hazardous Materials*, *142*, 144–152.
Gode, F., Atalay, E. D., & Pehlivan, E. (2008). Removal of Cr(VI) from aqueous solutions using modified red pine sawdust. *Journal of Hazardous Materials*, *152*, 1201–1207.
Guo, X. Y., Zhang, S., & Shan, X. Q. (2008). Adsorption of metal ions on lignin. *Journal of Hazardous Materials*, *151*, 134–142.
Herbelin, A., & Westall, J. (1999). *FITEQL, A computer program for determination of chemical equilibrium constants from experimental data. Version 4. 0*. Corvallis, OR: Department of Chemistry, Oregon State University.
Khan, M. N., & Wahab, M. F. (2006). Characterization of chemically modified corncobs and its application in the removal of metal ions from aqueous solution. *Journal of Hazardous Materials*, *B141*, 237–244.
Kohler, M., Curtis, G. P., David, E., Meece, D. E., & Davis, J. A. (2004). Methods for estimating adsorbed uranium(VI) and distribution coefficients of contaminated sediments. *Environmental Science and Technology*, *38*, 240–247.
Lee, B. G. (2001). *Heavy metal ion sorption of unmodified and modified lignocellulosic fibers*. Ph.D. Dissertation, Madison, University of Wisconsin-Madison.

Marmier, N., & Fromage, F. (1999). Comparing electrostatic and nonelectrostatic surface complexation modeling of the sorption of lanthanum on hematite. *Journal of Colloid and Interface Science*, *212*, 252–263.

Montanher, S. F., Oliveira, E. A., & Rollemberg, M. C. (2005). Removal of metal ions from aqueous solutions by sorption onto rice bran. *Journal of Hazardous Materials*, *B117*, 207–211.

Naiya, T. K., Hattacharya, A. K., & Das, S. K. (2008). Adsorption of Pb(II) by sawdust and Neem Bark from aqueous solutions. *Environmental Progress*, *27*, 313–328.

Ngah, W. S. W., & Hanafiah, M. A. K. M. (2008). Removal of heavy metal ions from wastewater by chemically modified plant wastes as adsorbents: A review. *Bioresource Technology*, *99*, 3935–3948.

Ofomaja, A. E. (2008). Kinetic study and sorption mechanism of methylene blue and methyl violet onto mansonia (Mansonia altissima) wood sawdust. *Chemical Engineering Journal*, *143*, 85–95.

Ofomaja, A. E., & Unuabonah, E. I. (2011). Adsorption kinetics of 4-nitrophenol onto a cellulosic material, mansonia wood sawdust and multistage batch adsorption process optimization. *Carbohydrate Polymers*, *83*, 1192–1200.

Özacar, M., & Şengil, I. A. (2005). Adsorption of metal complex dyes from aqueous solutions by pine sawdust. *Bioresource Technology*, *96*, 791–795.

Ravat, C., Dumonceau, J., & Monteil-Rivera, F. (2000). Acid/base and Cu(II) binding properties of natural organic matter extracted from wheat bran, modeling by the surface complexation model. *Water Research*, *34*, 1327–1339.

Reddad, Z., Cerente, C., Andres, Y., & Clolrec, P. L. (2002). Modeling of single and competitive metal adsorption onto a natural polysaccharide. *Environmental Science and Technology*, *36*, 2242–2248.

Robinson, T., Chandran, B., Naidu, G. S., & Nigam, P. (2002). Studies on the removal of dyes from a synthetic textile effluent using barley husk in static-bath and in a continuous flow, packed-bed, reactor. *Bioresource Technology*, *85*, 43–49.

Robinson, T., Chandran, B., & Nigam, P. (2002). Removal of dyes from a synthetic textile dye effluent by biosorption on apple pomace and wheat straw. *Water Research*, *36*, 2824–2830.

Sciban, M., Radetic, B., Kevresan, Z. A., & Klašnja, M. (2007). Adsorption of heavy metals from electroplating wastewater by wood sawdust. *Bioresource Technology*, *98*, 402–409.

Shukla, A., Zhang, Y. H., Dubey, P., Margrave, J. L., & Shukla, S. S. (2002). The role of sawdust in the removal of unwanted materials from water. *Journal of Hazardous Materials*, *B95*, 137–152.

Shukla, S. R., & Pai, R. S. (2005). Adsorption of Cu(II) Ni(II) and Zn(II) on modified jute fibres. *Bioresource Technology*, *96*, 1430–1438.

Singh, K. K., Rastogi, R., & Hasan, S. H. (2005). Removal of cadmium from waste water using agricultural waste using rice polish. *Journal of Hazardous Materials*, *A121*, 51–58.

Sposito, G. (1998). On points of zero charge. *Environmental Science and Technology*, *32*, 2815–2819.

Sud, D., Mahajan, G., & Kaur, M. P. (2008). Agricultural waste material as potential adsorbent for sequestering heavy metal ions from aqueous solutions – A review. *Bioresource Technology*, *99*, 6017–6027.

Tejado, A., Pen, C., Labidi, J., Echeverria, J. M., & Mondragon, I. (2007). Physicochemical characterization of lignins from different sources for use in phenol–formaldehyde resin synthesis. *Bioresource Technology*, *98*, 1655–1663.

Westall, J. C., Jones, J. D., & Gary, D. (1995). Models for association of metal ions with heterogeneous environmental sorbents. 1. Complexation of Co(II) by leonardite humic acid as a function of pH and $NaClO_4$ Concentration. *Environmental Science and Technology*, *29*, 951–959.

Yasemin, B., & Zek, T. (2007). Removal of heavy metals from aqueous solution by sawdust adsorption. *Journal of Environmental Sciences*, *19*, 160–166.

Ye, J. H., Dong, J. J., Lu, J. L., Zheng, X. Q., Jin, J., Chen, H., & Liang, Y. R. (2010). Effect of graft copolymerization of fir sawdust lignocellulose with N-vinylpyrrolidone on adsorption capacity to tea catechins. *Carbohydrate Polymers*, *81*, 441–447.